

# LOOKUP TABLES FOR PHASE RANDOMISATION IN HARDWARE GENERATED HOLOGRAMS

APRIL 9, 2020

Peter J. Christopher<sup>1,\*</sup> and Timothy D. Wilkinson<sup>1</sup>

<sup>1</sup>Centre of Molecular Materials, Photonics and Electronics, University of Cambridge, UK  
\*pjc209@cam.ac.uk

## ABSTRACT

The rise in virtual and mixed reality systems has prompted a resurgence of interest in two-dimensional and three-dimensional real-time computer generated holography. Phase randomisation is an integral part of holographic projection as it ensures independence in sub-frame techniques and reduces the edge enhancement seen in flat-phase images. Phase randomisation requires, however, the availability of a pseudo-random number generator as well as trigonometric functions such as  $\cos$  and  $\sin$ . On embedded devices such as field programmable gate arrays and digital signal processors this can be an unacceptable load and necessitate the use of proprietary intellectual property cores. Lookup tables are able to reduce the computational load but can run to many megabytes for even low-resolution systems.

This paper introduces the use of lookup tables (LUTs) in the context of two common algorithms used for real-time holographic projection: Gerchberg-Saxton and One-Step Phase-Retrieval. A simulated study is carried out to investigate the use of relatively small lookup tables where random numbers are repeated in sequence. We find that the increase in error is low and tunable to under 5% even for small look up tables. This results is also demonstrated experimentally. Finally, the implications of this study are discussed and conclusions drawn.

**Keywords** Computer Generated Holography · Holographic Video · Lookup Tables · Time-Multiplexed · Phase Randomisation

## 1 INTRODUCTION

The decades since the first computer generated holograms (CGHs) have seen a rapid growth in their quality and application. Holograms are now widely used in technologies including displays [1, 2], projectors [3, 4, 5], lithography [6], telecommunications [7], beam shaping [8], imaging [9, 10] and optical tweezing [11, 12]. While early research focussed primarily on producing still frames for display on spatial light modulators (SLMs), recent years have seen significant research in two newer areas, real-time video and three-dimensional (3D) displays [13]. Combined with the improvement in quality of available SLMs as well as an increase in user expectations of image quality have led to a computational problem orders of magnitude greater than that faced previously. Recent years have seen numerous efforts to tackle this including extensive use of Graphical Processing Units (GPUs), Field Programmable Gate Arrays (FPGAs) and Digital Signal Processors (DSPs).

This paper seeks to present a method of improving the speed of hologram generation for two common hologram generation algorithms - Gerchberg-Saxton (GS) and One-Step Phase-Retrieval (OSPR) - in the context of embedded devices including FPGAs and DSPs. This is done by moving elements of the computation dependent on a random number generator to a look-up table (LUT). We show that this can remove the need for trigonometric functions and a pseudo random number generator (PRNG) from the embedded process at the expense of higher memory usage. We also show that significant reuse of the random data can occur in each frame before significant error is introduced. This is then demonstrated on an implementation of OSPR for a  $1024 \times 1024$  binary ferroelectric display [14].

## 2 BACKGROUND

Figure 1 shows the setup of a phase insensitive holographic system. A light field is passed through a SLM known as the diffraction field (DF). The SLM applies a modulation or aperture function to the light that then propagates in free space before being scattered off of a diffuse screen. Depending on the ratio of propagation distance to SLM aperture size, this behaviour can be modelled as a Fourier or Fresnel transform. For constant illumination, planar wavefronts passed through a 100% fill factor pixellated SLM, the far-field hologram displayed are given by the Discrete Fourier Transform (DFT) [15],

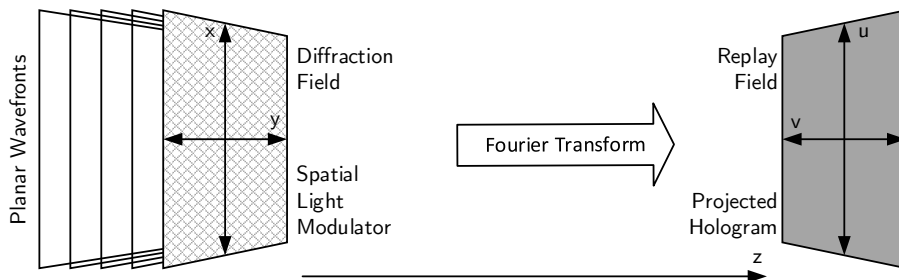


Figure 1: Coordinate systems used in describing a hologram.

$$F_{u,v} = \mathcal{F}\{f_{x,y}\} = \frac{1}{\sqrt{N_x N_y}} \sum_{x=0}^{N_x-1} \sum_{y=0}^{N_y-1} f_{xy} e^{-2\pi i \left( \frac{ux}{N_x} + \frac{vy}{N_y} \right)} \quad (1)$$

$$f_{x,y} = \mathcal{F}^{-1}\{F_{u,v}\} = \frac{1}{\sqrt{N_x N_y}} \sum_{u=0}^{N_x-1} \sum_{v=0}^{N_y-1} F_{uv} e^{2\pi i \left( \frac{ux}{N_x} + \frac{vy}{N_y} \right)}, \quad (2)$$

where  $x$  and  $y$  represent the source coordinates and  $u$  and  $v$  represent the spatial frequencies. Computational performance of  $O(N_x N_y \log N_x N_y)$  where  $N_x$  and  $N_y$  are the  $x$  and  $y$  respective resolutions can be achieved using the Fast Fourier Transform (FFT) algorithm [16, 17]. Finding a given far-field hologram can be taken as the problem of finding discrete aperture function where  $f(x, y)$  where  $F(u, v) = \mathcal{F}\{f(x, y)\}$ .

The majority of hologram generation algorithms begin by taking target complex replay field  $R$  and back propagating it to the diffraction field  $H = \mathcal{F}^{-1}\{R\}$  [18, 19]. The hologram is then modulated or *quantised* to conform to the constraints of the SLM. Normally this is done by changing the value of each pixel  $H_{x,y}$  to the nearest acceptable value  $H'_{x,y}$ . This is the *initial hologram*. Different algorithms then take different approaches to changing pixels within the modulation constraints in order to reduce the error of the new replay field  $R' = \mathcal{F}\{H'\}$ . [20]

Many applications are phase insensitive and generation algorithms can focus solely on matching target amplitudes. In this case two algorithms dominate, Gerchberg-Saxton (GS) and One-Step Phase-Retrieval (OSPR) shown in Figures 2 (left) and 2 (right) respectively [21, 22].

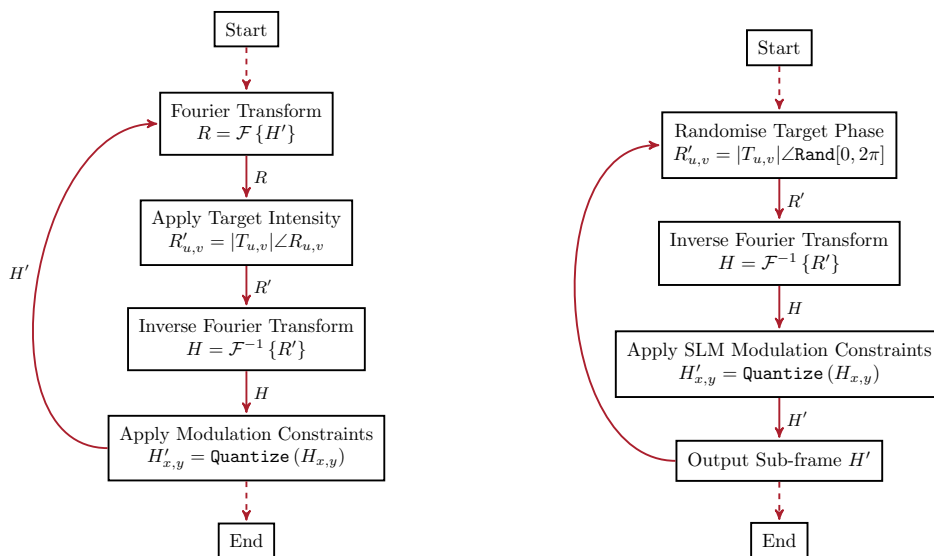


Figure 2: Gerchberg-Saxton algorithm (left) and One-Step Phase-Retrieval algorithm (right).

### 3 PHASE RANDOMISATION

The phase randomisation shown in Figures 2 (left) and 2 (right) for GS and OSPR is introduced for two primary reasons.

Firstly, adding random phase on the target image will diffuse the object light, enabling not only the high frequency component, but also the low frequency component being recorded on the hologram plane. More information will be preserved on the hologram plane. This has the effect of preventing edge enhancement [23].

Secondly, OSPR introduces phase randomisation to ensure speckle independence of the each reconstructed target sub-frames [2]. Time averaging then ensures a reduction in Mean Squared Error (MSE).

### 4 MOTIVATION

Software implementations of these algorithms are able to use PRNGs [24] and trigonometric functions to carry out the phase randomisation. Field Programmable Gate Arrays (FPGAs) or Digital Signal Processors (DSPs) are also capable of this but can require the use of proprietary IP cores for the PRNG and trigonometric functions. To improve performance, Lookup Tables (LUT) can be used. Random numbers can be generated at compile time to fill the LUT which then acts as a *pool* of random numbers for algorithms to sequentially draw from. If the length of the random number LUT is given by  $N_{LUT}$  then the case where  $N_{LUT}$  is greater than the size of the test image is indistinguishable from the case without a LUT. LUTs of this size can be impractical on low-cost devices [25].

### 5 RESULTS

Figure 3 shows an example of phase randomisation using LUTs. The *pool* of random numbers available from the LUT is cycled through sequentially with successive frames and sub-frames continuing from where the previous left off.

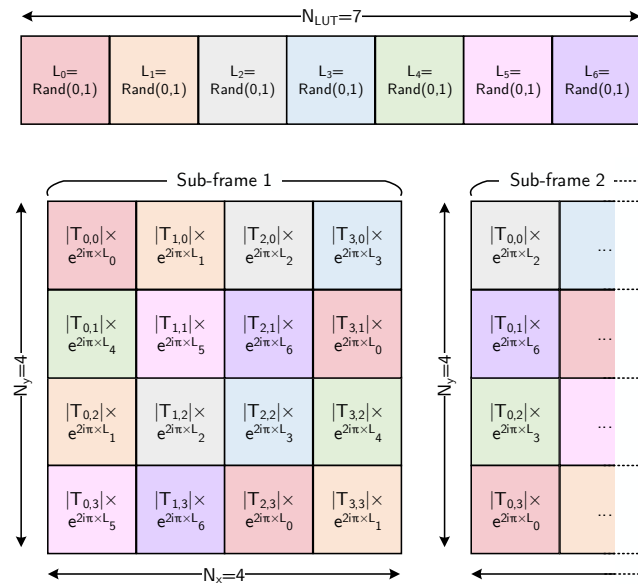


Figure 3: Example of phase randomisation using look-up tables, each block represents a single pixel.

This paper presents a heuristic approach for investigating the effect of  $N_{LUT}$  on edge enhancement and sub-frame independence. This is then tested on a binary phase ferroelectric device.

#### 5.1 Hard limits

For the sub-frame independence and edge enhancement reduction motivations, hard limits exist for theoretical correspondence between the LUT and pseudo-random number generator approaches.

The hard limit for  $N_{LUT}$  to meet the sub-frame independence constraint is that  $N_{LUT}$  must be greater than  $N_{SF}$ , where  $N_{SF}$  is the number of OSPR sub-frames.

To meet the edge enhancement constraint for both OSPR and GS, to ensure the hardware LUT approach is equivalent to the software pseudo-random number generator case,  $N_{LUT}$  must be at least equal to  $N_x N_y N_{SF}$  where  $N_x$  and  $N_y$  are the  $x$  and  $y$



Figure 4: Standard test images from the USC-SIPI image database.[26] From left to right: Mandrill, Peppers, Man, CameraMan, Aerial, Landscape

resolutions respectively. This is impractical on many hardware devices so instead we attempt to determine the relationship between phase randomisation LUT length and final error.

## 5.2 Results

Figure 5 shows the time averaged errors for prime values of  $N_{LUT}$  for OSPR binary phase holograms with 24 sub-frames for the six  $256 \times 256$  pixel test images shown in Figure 4. A LUT for this would require over 12 Mb of space and realtime generation on a 60 FPS device would require multiple GFLOPs of processing power. Prime values of  $N_{LUT}$  are used in order to avoid factorisation issues. Each error value shown is the average of 100 independent runs and is normalised to the mean error for the *Mandrill* test image to give the Normalised MSE (NMSE).

$$NMSE_{image,n} = MSE_{image,n} \frac{MSE_{Mandrill,1000}}{MSE_{image,1000}} \quad (3)$$

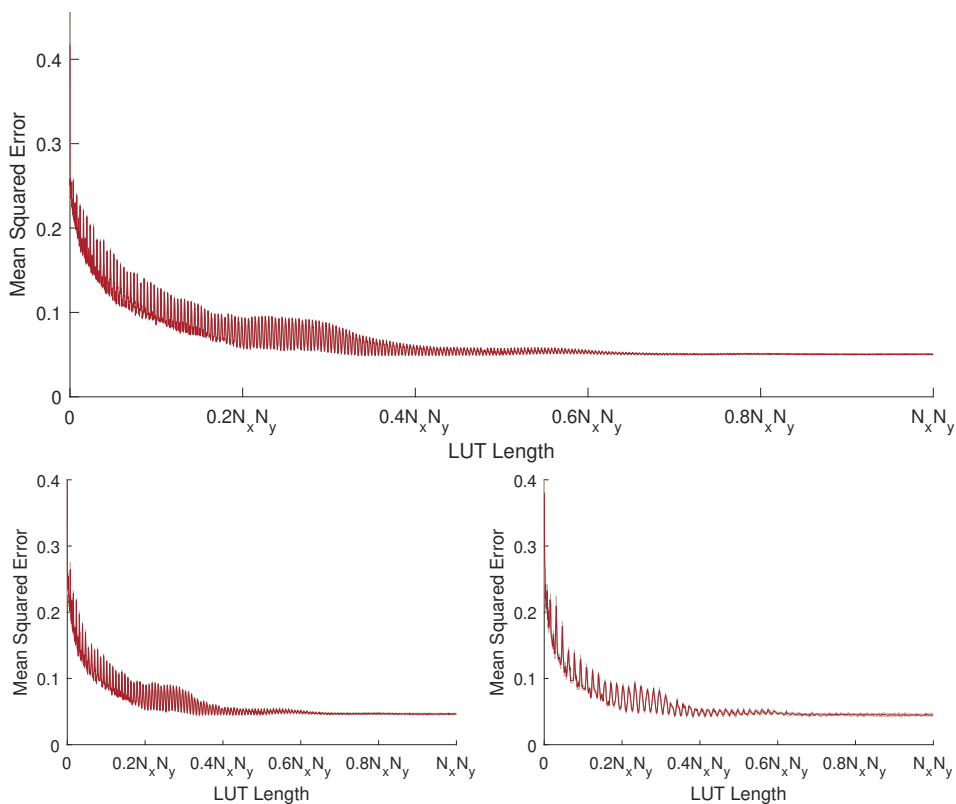


Figure 5: Time averaged errors for prime values of  $N_{LUT}$  for OSPR binary phase holograms with 24 sub-frames for the  $256 \times 256$  pixel test images shown in Figure 4. Each value is the average of 100 independent runs for each of the 6 test images. The mean value is shown in red with two standard deviations above and below shown in grey. A comparison with  $128 \times 128$  (bottom left) and  $64 \times 64$  (bottom right) holograms is shown for comparison.

The results show that, as expected, error is very high when  $N_{LUT}$  is 0 and drops off rapidly until  $N_{LUT} > N_{SF}$ . Descent is slower there after with significant variation. Spikes occur at regular intervals when the LUT would be close in length to a multiple of the resolution. For example  $N_{LUT} = 256$  leads to a sharp increase in error as every image row has the same phase behaviour.

Figure 5 also shows the effect of varying the hologram size  $N_x \times N_y$ . The similarity between the graphs suggests that for a given target error the required LUT size will be proportional to the total hologram size.

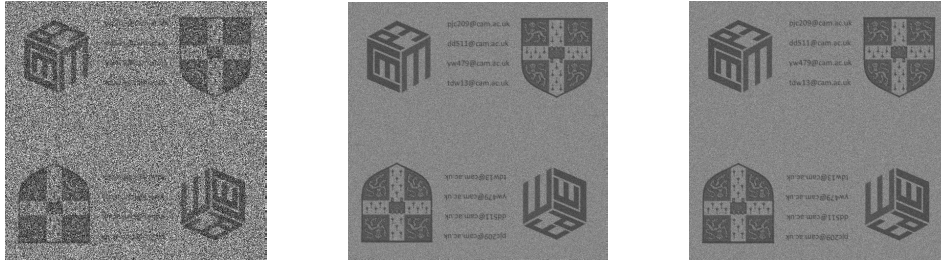


Figure 6: Single OSPR sub-frame (left) with time average of 24 OSPR sub-frames with independent phase randomisation (centre) and  $N_{LUT} = 10007$  (right). The right hand image demonstrates less than 5% additional error to the centre image.

Figure 6 shows this effect on a real image. A single OSPR frame is shown right with 24 sub-frames in the centre. Both of these are with independent random numbers. The right hand image shows the case of  $N_{LUT} = 10007$ , less than 0.03% of the naïve length, and shows less than 5% additional error. The value of 10007 for  $N_{LUT}$  was chosen as the first prime number larger than 10000 and similar results are seen for other large prime numbers. Independent trails with different test images showed no appreciable change in observed error. In practice the system admits of significant tuning for different test image resolutions as the oscillation in observed error is high in Figure 5.

## 6 VALIDATION



Figure 7: Top portion of the replay field for 24 OSPR time-averaged sub-frames with independent phase randomisation (left) and  $N_{LUT} = 10007$  (right). Captured using a Canon 5D Mark III with a 24-105mm lens and a  $1/60$  second exposure.

In order to validate our findings, we demonstrate the algorithm for a  $1024 \times 1024$  binary ferroelectric display as shown in Figure 7. The left hand image shows a fully independent randomisation while the right shows the case of  $N_{LUT} = 10007$ , less than 0.03% of the naïve length. The value of 10007 for  $N_{LUT}$  was chosen as the first prime number larger than 10000 and similar results are seen for other large prime numbers. Independent trails with different test images showed no appreciable change in observed error.

## 7 PERFORMANCE DISCUSSION

This paper has presented a simple method for removing the requirement for PRNGs and trigonometric functions from FPGA implementations of CGH. The process has the advantage of requiring only a single look-up operation. As the LUT is read through cyclically, the memory location can be predetermined, improving performance at runtime. This performance benefit comes at the cost of reduced runtime flexibility and a larger LUT size.

For comparison, a fast PRNG approach such as M-sequences would offer a small algebraic overhead and still require the use of LUTs for the sine and cosine terms.

For systems requiring runtime flexibility, PRNGs with LUTs for sin and cosine functions are expected to remain the dominant technique. For specific applications known at compile-time it is expected that this technique could offer performance and complexity benefits over existing approaches.

## 8 CONCLUSION

In this paper we initially reintroduced two reasons for phase randomisation in holographic projection: sub-frame independence and edge enhancement reduction. These have been discussed in the context of two algorithms: GS and OSPR. For embedded systems devices including FPGA and DSP these phase randomisation requirements can present a significant processing challenge and the use of LUTs can require many Mbs of storage for even small images

As a result of this we have proposed that a LUT can be used. We also put forward three primary constraints on the minimum length of the LUT. First that the LUT have a prime length to reduce the chance of matching the periodicity of the image. Second that the LUT have a length greater than the number of sub-frames and third that the LUT should be greater than the largest dimension of the image. For the case of using a Gerchberg-Saxton (GS) algorithm, only the first and third constraints apply.

The proposed method was demonstrated using a LUT of length 10007 for a simulated cases, less than 0.03% of the length required for complete sub-frame independence. These both conformed to our expectations with the simulated image showing little less than 5% additional error when using the LUT. Finally, we demonstrated this experimentally by generating frames for a binary phase projector. This also showed the expected behaviour with no visible quality differences when using a LUT of length 10007.

This result is of significance to embedded holographic systems as it negates the necessity for embedded complex number rotation operations and reduces the required computation and the overall implementation complexity. This comes at the cost of system flexibility.

## FUNDING

The authors would like to thank the Engineering and Physical Sciences Research Council (EP/L016567/1, EP/T008369/1 and EP/L015455/1) for financial support during the period of this research.

## DISCLOSURES

The authors declare no conflicts of interest.

## REFERENCES

- [1] Changwon Jang, Kiseung Bang, Gang Li, and ByoungHo Lee. Holographic Near-eye Display with Expanded Eye-box. *ACM Transactions on Graphics*, 37(6), 2018.
- [2] Andrew Maimone, Andreas Georgiou, and Joel S. Kollin. Holographic near-eye displays for virtual and augmented reality. *ACM Transactions on Graphics*, 36(4):1–16, 2017. ISSN 07300301. doi: 10.1145/3072959.3073624. URL <http://dl.acm.org/citation.cfm?doid=3072959.3073624>.
- [3] Michal Makowski, Izabela Ducin, Karol Kakarenko, Jaroslaw Suszek, Maciej Sypek, and Andrzej Kolodziejczyk. Simple holographic projection in color. *Optics Express*, 20(22):25130, 2012. doi: 10.1364/oe.20.025130.
- [4] Michal Makowski, Adam Kowalczyk, Marcin Bieda, Jaroslaw Suszek, Izabela Ducin, and Tomoyoshi Ito. Miniature Holographic Projector with Cloud Computing Capability. *Applied Optics*, 186(4):2282–2290, 2018. ISSN 0022-1767. doi: 10.4049/jimmunol.1003225.
- [5] Chenliang Chang, Yijun Qi, Jun Wu, Jun Xia, and Shouping Nie. Speckle reduced lensless holographic projection from phase-only computer-generated hologram. *Optics Express*, 25(6):6568, 2017. doi: 10.1364/oe.25.006568.
- [6] A. J. Turberfield, M. Campbell, D. N. Sharp, M. T. Harrison, and R. G. Denning. Fabrication of photonic crystals for the visible spectrum by holographic lithography. *Nature*, 404(6773):53–56, 2000. ISSN 00280836. doi: 10.1038/35003523. URL <http://www.nature.com/doifinder/10.1038/35003523>.
- [7] W. A. Crossland, T. D. Wilkinson, I. G. Manolis, M. M. Redmond, and A. B. Davey. Telecommunications applications of LCOS devices. *Molecular Crystals and Liquid Crystals Science and Technology Section A: Molecular Crystals and Liquid Crystals*, 375:1–13, 2002. ISSN 1058725X. doi: 10.1080/10587250210552.
- [8] Yanran Zhang, Chenliang Chang, Caojin Yuan, Shaotong Feng, Shouping Nie, and Jianping Ding. Composite generation of independently controllable multiple three-dimensional vector focal curve beams. *Optics Communications*, 450(June):296–303, 2019. ISSN 00304018. doi: 10.1016/j.optcom.2019.06.021. URL <https://doi.org/10.1016/j.optcom.2019.06.021>.
- [9] D. M. Sheen, D. L. McMakin, and T. E. Hall. Three-dimensional millimeter-wave imaging for concealed weapon detection. *IEEE Transactions on Microwave Theory and Techniques*, 49(9):1581–1592, 2001. ISSN 00189480. doi: 10.1109/22.942570.
- [10] Mehdi Daneshpanah, Susanne Zwick, Frederik Schaal, Michael Warber, Bahram Javidi, and Wolfgang Osten. 3D holographic imaging and trapping for non-invasive cell identification and tracking. *IEEE/OSA Journal of Display Technology*, 6(10): 490–499, 2010. ISSN 1551319X. doi: 10.1109/JDT.2010.2043499.

- [11] J. A. Grieve, A. Ulcinas, S. Subramanian, G. M. Gibson, M. J. Padgett, D. M. Carberry, and M. J. Miles. Hands-on with optical tweezers: a multitouch interface for holographic optical trapping. *Optics Express*, 17(5):3595, 2009. doi: 10.1364/oe.17.003595.
- [12] H. Melville, D.F. Milne, G.C. Spalding, W. Sibbett, K. Dholakia, and D. McGloin. Optical trapping of three-dimensional structures using dynamic holograms. *Optical Express*, 11(26):3562–3567, 2003.
- [13] Georges Nehmetallah and Partha P. Banerjee. Applications of digital and analog holography in three-dimensional imaging. *Advances in Optics and Photonics*, 4(4):472–553, 2012. doi: 10.1364/aop.4.000472.
- [14] Jonathan P. Freeman, Timothy D. Wilkinson, and Paul Wisely. Visor projected HMD for fast jets using a holographic video projector. In *Proc. SPIE*, volume 7690, page 76901H, 2010. ISBN 9780819481542. doi: 10.1117/12.855020. URL <http://proceedings.spiedigitallibrary.org/proceeding.aspx?doi=10.1117/12.855020>.
- [15] Joseph W Goodman. *Introduction to Fourier Optics*. Roberts & Co. Publishers, 3rd edition, 2005.
- [16] Matteo Frigo and Steven G. Johnson. The design and implementation of FFTW3. *Proceedings of the IEEE*, 93(2):216–231, 2005. ISSN 00189219. doi: 10.1109/JPROC.2004.840301.
- [17] Joel Carpenter and Timothy D. Wilkinson. Graphics processing unit-accelerated holography by simulated annealing. *Optical Engineering*, 49(9):095801, 2010. ISSN 0091-3286. doi: 10.1117/1.3484950.
- [18] Jae Hyeung Park. Recent progress in computer-generated holography for three-dimensional scenes. *Journal of Information Display*, 18(1):1–12, 2017. ISSN 21581606. doi: 10.1080/15980316.2016.1255672. URL <https://doi.org/10.1080/15980316.2016.1255672>.
- [19] Peter Wai Ming Tsang and Ting Chung Poon. Review on the State-of-the-Art Technologies for Acquisition and Display of Digital Holograms. *IEEE Transactions on Industrial Informatics*, 12(3):886–901, 2016. ISSN 15513203. doi: 10.1109/TII.2016.2550535.
- [20] Peter J. Christopher, Jamie D. Lake, Daoming Dong, Hannah J. Joyce, and Timothy D. Wilkinson. Improving holographic search algorithms using sorted pixel selection. *J. Opt. Soc. Am. A*, 36(9):1456–1462, Sep 2019. doi: 10.1364/JOSAA.36.001456. URL <http://josaa.osa.org/abstract.cfm?URI=josaa-36-9-1456>.
- [21] R. W. Gerchberg and W. O. Saxton. A practical algorithm for the determination of phase from image and diffraction plane pictures. *Optik*, 35:237–246, 1972. ISSN 1063-7818. doi: 10.1070/qe2009v039n06abeh013642.
- [22] A. J. Cable, E. Buckley, P. Mash, N. A. Lawrence, T. D. Wilkinson, and W. A. Crossland. Real-time Binary Hologram Generation for High-quality Video Projection Applications. In *SID Symposium Digest of Technical Papers*, volume 35, pages 1431–1433, 2004. doi: 10.1889/1.1825772.
- [23] Tomoyoshi Shimobaba, Takashi Kakue, and Tomoyoshi Ito. Real-time and low speckle holographic projection. *Proceeding - 2015 IEEE International Conference on Industrial Informatics, INDIN 2015*, 1(1):732–741, 2015. doi: 10.1109/INDIN.2015.7281827.
- [24] Tomoyoshi Shimobaba and Tomoyoshi Ito. Random phase-free computer-generated hologram. *Optics Express*, 23(7):9549–9554, 2015. doi: 10.1364/OE.23.009549. URL <http://dx.doi.org/10.1364/OE.23.009549>.
- [25] Tomoyoshi Shimobaba, Takashi Kakue, and Tomoyoshi Ito. Review of Fast Algorithms and Hardware Implementations on Computer Holography. *IEEE Transactions on Industrial Informatics*, 12(4):1611–1622, 2016. ISSN 15513203. doi: 10.1109/TII.2015.2509452.
- [26] USC-SIPI Database. [www.sipi.usc.edu/database/](http://www.sipi.usc.edu/database/), 2018-01-01. URL <http://www.sipi.usc.edu/database/>.